

Photon statistics of atomic fluorescence after π -pulse excitation

Kazuyoshi Yoshimi¹ and Kazuki Koshino^{1,2}

¹College of Liberal Arts and Sciences, Tokyo Medical and Dental University, Ichikawa, Chiba 272-0827, Japan

²PRESTO, Japan Science and Technology Agency, Kawaguchi, Saitama 332-0012, Japan

(Received 2 July 2010; published 17 September 2010)

The photon statistics of atomic fluorescence after π -pulse excitation is investigated in a system in which the input and output ports are connected to an atom. Since spontaneous decay during input pulse excitation occurs, the output pulse generally contains a multiphoton component with a certain probability. We quantitatively evaluate the probability of the output pulse containing multiple photons and determine the conditions for ideal single-photon generation.

DOI: [10.1103/PhysRevA.82.033818](https://doi.org/10.1103/PhysRevA.82.033818)

PACS number(s): 42.50.Ar, 42.65.Sf, 32.50.+d, 33.80.-b

I. INTRODUCTION

Generation of single photons on demand is a key topic in quantum information technology, since photons have long quantum coherence times, which are required for qubits [1–4]. Indeed, some experiments have succeeded in constructing quantum gates by controlling a photon by another photon through a nonlinear medium [5–7]. A two-level quantum system (hereafter, referred to as an atom) is generally used to generate single photons [8–10]. The basic strategy is given by the following process: (i) A classical π pulse is input to induce an atomic transition from the initial ground state to the excited state. (ii) After excitation, a photon is emitted to the output port due to spontaneous decay to the ground state. By repeating these steps, it is expected to be possible to generate single photons on demand. However, spontaneous decay also occurs during π -pulse excitation in actual processes. This causes undesirable *multiphoton* generation with a certain probability [11,12].

The aim of this paper is to determine the conditions for ideal single-photon generation in a system that has two photon-propagation paths (i.e., input and output ports) that are connected to a two-level system (see Fig. 1). In this system, emitted photons can be efficiently collected when the coupling to the output port is larger than that to the input port. Although this condition is advantageous for an ideal single-photon source, it also increases the probability of multiple-photon generation, since atomic fluorescence may be emitted to the output port during π -pulse excitation. To evaluate multiple-photon generation, we investigate the photon statistics of atomic fluorescence after π -pulse excitation using a quantum multimode formalism in which both the atomic system and the photon fields are quantized and the multimode nature of the photon field is precisely accounted for [13]. We analytically derive the equations of motion for the multipoint functions and numerically calculate the multipoint functions and the multiple-photon probabilities over a wide range of parameters. Finally, we determine the conditions for single-photon generation.

II. FORMULATION

A. Model

Figure 1 schematically depicts the physical setup considered in this paper. A two-level system (atom) is coupled to two

semi-infinite one-dimensional optical paths (ports A and B). A classical π pulse is input from port A to excite the atom. Port B is used as the output port, into which radiation from the atom is predominantly forwarded. The radiative decay rates of the atom to ports A and B are denoted by Γ_a and Γ_b , respectively. For simplicity, we neglect the loss here, assuming recent low-loss setups realized in several experiments [14,15] (the loss from the atom, such as radiation to the environment and nonradiative decay can be modeled by introducing another port coupled to the atom, as discussed in Appendix B). Setting $\hbar = c = 1$, the Hamiltonian under the rotating-wave approximation is given by

$$\mathcal{H} = \Omega \sigma^\dagger \sigma + \int dk [ka_k^\dagger a_k + kb_k^\dagger b_k] + (i\sqrt{\Gamma_a} \sigma^\dagger \tilde{a}_{r=0} + i\sqrt{\Gamma_b} \sigma^\dagger \tilde{b}_{r=0} + \text{H.c.}), \quad (1)$$

where Ω is the atomic transition energy and σ is the atomic lowering operator. a_k and b_k denote photonic annihilation operators for a wave number k in ports A and B, respectively. The real-space representations of a_k and b_k are defined by $\tilde{a}_r = (2\pi)^{-1/2} \int dk a_k e^{ikr}$ and $\tilde{b}_r = (2\pi)^{-1/2} \int dk b_k e^{ikr}$, respectively. The atom interacts radiatively with the two ports at $r = 0$, as shown in Fig. 1. Therefore, the $r < 0$ and $r > 0$ regions, respectively, represent the incoming and outgoing fields.

B. Input and output states

Next, we describe the initial-state vector of the overall system. The atom is initially in the ground state. A classical π pulse is input from the $r < 0$ region of port A, whereas no photon is input from port B. The input state vector is then given by

$$|\Phi_i\rangle = \mathcal{N} \exp \left[\int dr E(r) \tilde{a}_r^\dagger \right] |0\rangle, \quad (2)$$

where $E(r)$ is the amplitude of the input π pulse [see Eq. (8) for its detailed form], $\mathcal{N} = \exp[-\int dr |E(r)|^2/2]$ is the normalization constant, and $|0\rangle$ is the overall ground state (the product of the photonic vacuum and atomic ground-state vectors).

The atom is excited by this input pulse, and decays to the ground state by emitting photons into ports A and B. We choose the final moment t to be an arbitrary large time at which the

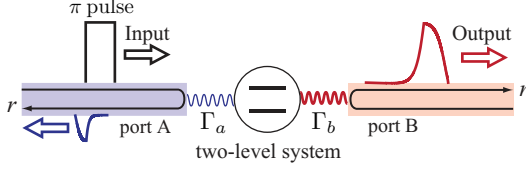


FIG. 1. (Color online) Schematic of the physical setup. A two-level system is coupled to ports A and B with the radiative decay rates Γ_a and Γ_b , respectively. A classical π pulse is input from port A for excitation. Port B is used as the output port as radiation from the atom is predominantly transferred to it.

atom is completely deexcited. The final state vector is related to the initial one by the Schrödinger equation as $|\Phi_f(t)\rangle = e^{-i\hat{H}t}|\Phi_i\rangle$. The t dependence of $|\Phi_f(t)\rangle$ is inessential for sufficiently large t , since it describes the translational motion of outgoing photons. The final-state vector can formally be written as

$$|\Phi_f(t)\rangle = \sum_{n=0}^{\infty} |\psi_n(t)\rangle, \quad (3)$$

where $|\psi_n(t)\rangle$ represents a state vector for which n photons are emitted to port B,

$$|\psi_n(t)\rangle = \sum_{m=0}^{\infty} \int \frac{d^m \xi d^n \mathbf{r}}{\sqrt{m!n!}} g_{mn}(\mathbf{r}, \xi; t) \tilde{a}_{\xi_1}^\dagger \cdots \tilde{a}_{\xi_m}^\dagger \tilde{b}_{r_1}^\dagger \cdots \tilde{b}_{r_n}^\dagger |0\rangle, \quad (4)$$

where g_{mn} denotes a part of the output wave function, which contains $m+n$ photons (m photons in port A and n photons in port B). The probability that n photons are emitted to port B is given by

$$P_n(t) = \langle \psi_n(t) | \psi_n(t) \rangle = \sum_{m=0}^{\infty} \int d^m \xi d^n \mathbf{r} |g_{mn}(\mathbf{r}, \xi; t)|^2. \quad (5)$$

$$C_m(\mathbf{r}_m; t) = \begin{cases} \frac{\pi^2 \Gamma_b}{2d^2(\lambda_+ - \lambda_-)} \left[-\frac{1 - e^{\lambda_+(t - r_{m-1})}}{\lambda_+} + \frac{1 - e^{\lambda_-(t - r_{m-1})}}{\lambda_-} \right] C_{m-1}(\mathbf{r}_{m-1}; t), & 0 < t - r_{m-1} < t - r_m < d \\ C_m(\mathbf{r}_m; t)|_{r_m=t-d} \exp[-\Gamma(t - d - r_m)], & 0 < t - r_{m-1} < d < t - r_m, \\ 0, & d < t - r_{m-1} < t - r_m \end{cases} \quad (9)$$

where $\Gamma = \Gamma_a + \Gamma_b$ and we have set $r_1 > \cdots > r_m$ without loss of generality. The eigenfrequencies λ_{\pm} are given by

$$\lambda_{\pm} = -\frac{3\Gamma}{4} \pm i\sqrt{\frac{\pi^2}{d^2} - \frac{\Gamma^2}{16}}. \quad (10)$$

Since $C_0 = 1$ by definition, $C_m(\mathbf{r}_m; t)$ can be obtained iteratively. The fact that C_m ($m \geq 2$) is nonvanishing implies that more than two photons may appear in the output pulse.

The objective of this paper is to determine the conditions for obtaining only one photon in the output, namely, $P_n \sim \delta_{n,1}$,

Note that the norms of g_{mn} satisfy the sum rule of $\sum_{m,n} \int d^m \xi d^n \mathbf{r} |g_{mn}(\mathbf{r}, \xi; t)|^2 = \sum_n P_n(t) = 1$. Hereafter, we refer to the photons emitted to port B as the *output* photons.

C. Photon statistics

The output photon statistics are given by P_n ($n = 0, 1, \dots$). To calculate P_n , we introduce the m -point intensity correlation functions defined by

$$C_m(\mathbf{r}_m; t) \equiv \langle \Phi_f(t) | \tilde{b}_{r_1}^\dagger \cdots \tilde{b}_{r_m}^\dagger \tilde{b}_{r_m} \cdots \tilde{b}_{r_1} | \Phi_f(t) \rangle, \quad (6)$$

where $\mathbf{r}_m \equiv (r_1, \dots, r_m)$ denotes the m spatial coordinates of m photons in port B. The norms of the correlation functions $I_m(t) = \int d^m \mathbf{r}_m C_m(\mathbf{r}_m; t)$, are related to P_n by

$$I_m(t) = \sum_{k=m}^{\infty} \frac{k!}{(k-m)!} P_k(t). \quad (7)$$

The procedure for determining P_n is as follows. We derive analytic expressions for $C_m(\mathbf{r}_m; t)$ and evaluate $I_m(t)$ numerically for small m . (Typically, calculating up to I_4 is sufficient for our purpose, since I_4 becomes negligibly small for π -pulse excitation.) We then obtain $P_m(t)$ from Eq. (7) with high accuracy. The details are described in Sec. III B.

III. RESULTS

In this section, we numerically characterize the output pulse in terms of the spatial shape and the photon statistics. The input π pulse $E(r)$ is chosen to be a single rectangle pulse with a pulse length d and a central frequency ω :

$$E(r) = \begin{cases} \frac{\pi}{2d\sqrt{\Gamma_a}} \exp(i\omega r), & -d < r < 0 \\ 0, & \text{otherwise} \end{cases}. \quad (8)$$

The pulse amplitude $E_0 \equiv \pi/(2d\sqrt{\Gamma_a})$ is adjusted based on the pulse length d . This pulse induces complete excitation of the atom when radiative damping of the atom is assumed to be absent. For this input π pulse, the m -point function $C_m(\mathbf{r}_m; t)$ is given by (see Appendix A for derivation)

where $\delta_{i,j}$ is the Kronecker delta. In particular, we study the dependence of the photon statistics on the input pulse length d . Hereafter, we take Γ_a^{-1} as the unit of time by setting $\Gamma_a = 1$, and we focus on the resonant input ($\omega = \Omega$).

A. Pulse profile

We first discuss the spatial profile of the output pulse that is characterized by $C_1(r; t) = \langle \tilde{b}_r^\dagger(t) \tilde{b}_r(t) \rangle$. As mentioned earlier, $C_1(r; t)$ becomes a function of only one variable $t - r$ if

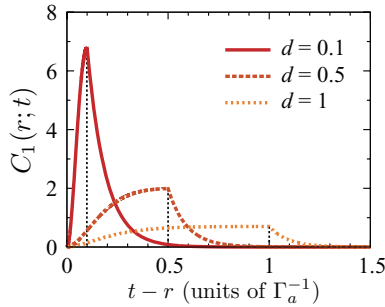


FIG. 2. (Color online) The spatial profile of the pulse. The input pulse length d is chosen at $0.1\Gamma_a^{-1}$ (solid line), $0.5\Gamma_a^{-1}$ (dashed line), and Γ_a^{-1} (dotted line) at $\Gamma_b/\Gamma_a = 10$.

t is sufficiently large. In Fig. 2, by setting $\Gamma_b = 10 \gg \Gamma_a$, $C_1(r; t)$ is plotted for several input pulse lengths d . C_1 increases monotonically in the $0 < t - r < d$ region, since the atomic excitation increases during π -pulse excitation. In contrast, C_1 decreases monotonically in the $d < t - r$ region, since the atom decays radiatively without being excited. In Secs. III B and III C, we calculate the multiple-photon probabilities and determine the condition for single-photon generation.

B. Photon statistics

In this section, we investigate the photon statistics of the output pulse. Figure 3(a) shows the norms of the multipoint functions (I_1 , I_2 , and I_3) as functions of the pulse length d . $I_1 (= \sum_{k=1}^{\infty} k P_k)$, which represents the average photon number in the output pulse, is approximately unity for a short pulse ($d \ll 1$), whereas it approaches zero for a long pulse ($d \gg 1$). This behavior is understood by the following considerations. In the short-pulse limit, the input π pulse can be considered to induce instantaneous complete excitation of the atom. The atomic excitation is converted into a single photon, which is forwarded to ports A and B with ratios of Γ_a/Γ and Γ_b/Γ , respectively. This assumption reproduces the value of $I_1 \sim \Gamma_b/\Gamma \sim 0.91$ well in the short-pulse region of Fig. 3(a). The increase in d gives rise to two effects: generation of more than two photons and incomplete π -pulse excitation. Thus, as d increases from the short-pulse limit, I_1 , I_2 , and I_3 initially increase due to the former effect and then decrease due to the latter effect.

Next, we show the photon statistics for the output pulse. As observed in Fig. 3(a), the values of I_m rapidly approach zero as m increases. Therefore, we can evaluate the values of P_n by setting $I_m = 0$ for $m \geq 4$. Then, from Eq. (7), we have $P_1 = I_1 - I_2 + I_3/2$, $P_2 = (I_2 - I_3)/2$, $P_3 = I_3/6$, and $P_m = 0$ for $m \geq 4$. Figure 3(b) shows a plot of P_n as a function of d . Ideal single-photon generation $P_n \sim \delta_{n,1}$ is achieved in the short-pulse limit ($d \ll 1$). The ratio between P_1 and P_0 is approximately given by $P_1/P_0 = \Gamma_b/\Gamma_a$ for $d \ll 1$. As d increases, P_1 (P_0) decreases (increases) and approaches 0 (1) for $d \gg 1$ because the π -pulse excitation becomes incomplete. The two-photon probability P_2 increases around $d = 1$ and has a maximum value of about 0.1. In other words, when the pulse length is comparable to the lifetime of the atom, the output pulse contains a multiple-photon component with a

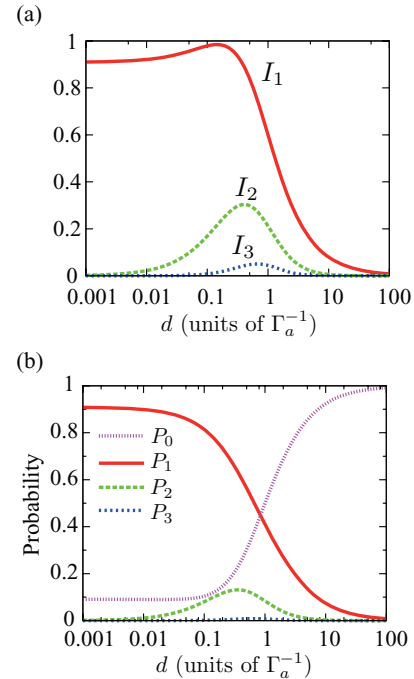


FIG. 3. (Color online) The pulse-length dependences of (a) I_i ($i = 1, 2, 3$) and (b) P_i ($i = 0, 1, 2, 3$), where $\Gamma_b = 10$.

high probability. The three-photon probability P_3 is negligible at all pulse lengths.

C. Conditions for single-photon generation

Before discussing the conditions for single-photon generation ($P_n \sim \delta_{n,1}$), we observe that there are two characteristic frequencies that govern photon generation in the present setup. They are obtained by dividing λ_{\pm} into two components: $\lambda_D \equiv 3\Gamma/4$ and $\lambda_R \equiv \sqrt{\pi^2/d^2 - \Gamma^2/16}$ [see Eq. (10)]. The former determines the time scale of atomic decay, and the latter determines the time scale of atomic excitation by the input pulse, which coincides with the Rabi frequency π/d in the short-pulse limit of $d \ll 1$.

The condition for ideal single-photon generation involves two factors. (i) The multiple-photon component P_2 should be suppressed. This component is most suppressed when the two time scales coincide (i.e., $\lambda_D = \lambda_R$). This equation can be recast as $d = \sqrt{8/5}\pi/\Gamma$, which becomes 0.361 for $\Gamma_b = 10$.

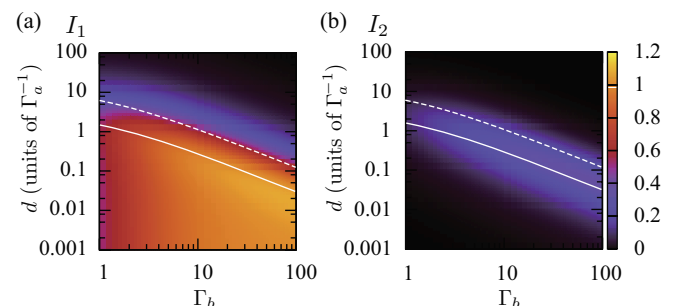


FIG. 4. (Color online) The integrals of (a) one-point function I_1 and (b) two-point function I_2 as functions of d and Γ_b . The white line (broken line) represents $d = \sqrt{8/5}\pi/\Gamma$ ($d = 4\pi/\Gamma$).

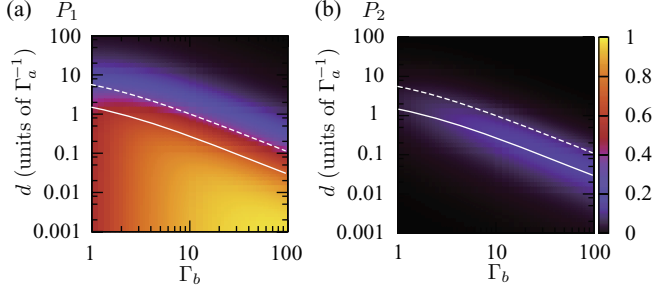


FIG. 5. (Color online) The probabilities of (a) single-photon and (b) two-photon states as functions of d and Γ_b . The white line (broken line) represents $d = \sqrt{8/5}\pi/\Gamma$ ($d = 4\pi/\Gamma$).

This value agrees well with the pulse length that maximizes P_2 , as shown in Fig. 2(b). (ii) The π -pulse excitation is complete, and the output pulse contains nearly one photon ($I_1 \sim 1$). Perfect excitation is achieved in the short-pulse limit where the atomic radiation during the π -pulse excitation is negligible. On the other hand, atomic excitation disappears in the long-pulse limit, as seen from Eq. (9): $C_1(r, t) = \Gamma_b \langle \sigma^\dagger(t) \sigma(t) \rangle \sim \pi^2 \Gamma_b / (d^2 \Gamma^2) (1 - e^{-\Gamma t/2})^2 \rightarrow 0$. The boundary between these two behaviors is characterized by $\lambda_R = 0$, which can be rewritten as $d = 4\pi/\Gamma \sim 1.14$ for $\Gamma_b = 10$. As seen from Fig. 3(b), this condition provides a good estimate for the pulse length above which the output photon number starts to decrease.

Based on these considerations, we clarify the conditions for single-photon generation. Figure 4 plots I_1 and I_2 as functions of d and Γ_b . The equalities $d = \sqrt{8/5}\pi/\Gamma$ and $d = 4\pi/\Gamma$ are also indicated by the solid and broken lines, respectively. Figure 4 shows that both I_1 and I_2 have broad peaks around the solid line. Thus, radiation to port B is most active when $d \sim \sqrt{8/5}\pi/\Gamma$. Figure 5 plots the photon statistics P_1 and P_2 as functions of d and Γ_b . P_2 has a broad peak around the solid line, whereas P_1 does not. This means that the peak of I_1 around the solid line is solely due to increasing multiple-photon generation. Therefore, $d_m = \sqrt{8/5}\pi/\Gamma$ gives the upper limit of the input pulse length for generating a single-photon state.

IV. SUMMARY

We have studied the photon statistics of atomic fluorescence after π -pulse excitation in a two-level system coupled to input and output ports. The equations of motion for multipoint functions have been analytically derived, and multipoint functions and multiple-photon probabilities were numerically calculated from them. It is demonstrated that single-photon generation becomes effective when the condition $d < \sqrt{8/5}\pi/\Gamma$ is satisfied, where atomic radiation during π -pulse excitation is considered to be negligible. This result is expected to provide a useful guide when constructing an ideal single-photon source for experiments.

ACKNOWLEDGMENTS

We thank Professor T. Kato for fruitful discussions. This research was partially supported by the Nakajima Foundation

and MEXT KAKENHI (Grants No. 22244035 and No. 211104507).

APPENDIX A: DERIVATION OF EQ. (9)

In this appendix, we derive analytical expressions for the multipoint functions for the output state. We also obtain an exact formula for the multipoint functions, where the input mode function is chosen as a classical π pulse given by Eq. (8).

First, we derive the input-output relations in the $0 < r < t$ region from the Heisenberg equations for the output field operators $\tilde{a}_r(t)$ and $\tilde{b}_r(r)$,

$$\tilde{a}_r(t) = \tilde{a}_{r-t}(0) - \sqrt{\Gamma_a} \sigma(t-r), \quad (\text{A1})$$

$$\tilde{b}_r(t) = \tilde{b}_{r-t}(0) - \sqrt{\Gamma_b} \sigma(t-r), \quad (\text{A2})$$

where $\tilde{a}_r(t)$ and $\tilde{b}_r(t)$ are the real-space representations of $a_k(t)$ and $b_k(t)$, respectively. Since the initial state is given by Eq. (2), we can obtain the following equations: $\tilde{a}_r(0)|\Phi_i\rangle = E(r)|\Phi_i\rangle$ and $\tilde{b}_r(0)|\Phi_i\rangle = 0$. By using the input-output relations, we obtain the Heisenberg equation for σ as

$$\frac{d}{dt} \sigma = -\frac{\Gamma}{2} \sigma - (2\sigma^\dagger \sigma - 1) [\sqrt{\Gamma_a} \tilde{a}_{-t}(0) + \sqrt{\Gamma_b} \tilde{b}_{-t}(0)], \quad (\text{A3})$$

where $\Gamma \equiv \Gamma_a + \Gamma_b$.

The m -point function for the output state in an output port is given by $C_m(\mathbf{r}_m; t) \equiv \langle \Phi_i(t) | \tilde{b}_{r_1}^\dagger \cdots \tilde{b}_{r_m}^\dagger \tilde{b}_{r_m} \cdots \tilde{b}_{r_1} | \Phi_i(t) \rangle$, where the spatial ordering is set as $r_1 > r_2 > \cdots > r_m$ without loss of generality. By using the input-output relation Eq. (A2) and the commutation relation $[\tilde{b}_r(0), \sigma(\tau)] = 0$ ($r < -\tau$) due to causality, $C_m(\mathbf{r}_m; t)$ can be rewritten as

$$C_m(\mathbf{t}_m) \equiv C_m(\mathbf{r}_m; t) = \Gamma_b^m \langle \sigma^\dagger(t_1) \cdots \sigma^\dagger(t_m) \sigma(t_m) \cdots \sigma(t_1) \rangle, \quad (\text{A4})$$

where $t_m = t - r_m$ and $\mathbf{t}_m \equiv (t_1, t_2, \dots, t_m)$. Thus, we can obtain $C_m(\mathbf{t}_m)$ by solving the atomic equation of motion. By using Eq. (B2), the equation of motion for $C_m(\mathbf{t}_m)$ under $0 < t_{m-1} < t_m$ is given by

$$\frac{d}{dt_m} C_m(\mathbf{t}_m) = -\Gamma C_m(\mathbf{t}_m) + 2E(-t_m) S_m(\mathbf{t}_m), \quad (\text{A5})$$

where $S_m(\mathbf{t}_m) \equiv \Gamma_b^m \langle \sigma^\dagger(t_1) \cdots \sigma^\dagger(t_{m-1}) \sigma(t_m) \cdots \sigma(t_1) \rangle$ obeys the following equation of motion:

$$\frac{d}{dt_m} S_m(\mathbf{t}_m) = -\frac{\Gamma}{2} S_m(\mathbf{t}_m) - E(-t_m) \times [2C_m(\mathbf{t}_m) - \Gamma_b C_{m-1}(\mathbf{t}_{m-1})]. \quad (\text{A6})$$

By definition, the initial conditions are given by $C_0(0) = 1$ and $S_0(0) = 0$, respectively.

When we choose $E(r)$ as a π pulse given by Eq. (8), the preceding simultaneous differential equations can be solved

analytically. In this case, $C_m(t_m)$ is given by

$$C_m(t_m) = \begin{cases} \frac{\pi^2 \Gamma_b}{2d^2(\lambda_+ - \lambda_-)} \left[-\frac{1 - e^{\lambda_+(t_m - t_{m-1})}}{\lambda_+} + \frac{1 - e^{\lambda_-(t_m - t_{m-1})}}{\lambda_-} \right] C_{m-1}(t_{m-1}), & 0 < t_{m-1} < t_m < d \\ C_m(t_m = d, t_{m-1}) \exp[-\Gamma(t_m - d)], & 0 < t_{m-1} < d < t_m, \\ 0, & d < t_{m-1} < t_m \end{cases}, \quad (\text{A7})$$

where $\lambda_{\pm} \equiv -3\Gamma/4 \pm (\Gamma^2/16 - \pi^2/d^2)^{1/2}$ is the eigenfrequency.

APPENDIX B: THE LOSS FROM THE ATOM

The loss from the atom can be taken into account by assuming an imaginary port as dealing the environment, into which the atom decays with a rate of Γ_c . The input-output relation for this port is given by

$$\tilde{c}_r(t) = \tilde{c}_{r-t}(0) - \sqrt{\Gamma_c} \sigma(t - r), \quad (\text{B1})$$

where $\tilde{c}_r(t)$ denotes a photonic annihilation operator for a real-space position r in the environment. The initial state is given by $\tilde{c}_r(0)|\Phi_i\rangle = 0$, since no photon is input from the

environment. By using the input-output relations of Eqs. (A1), (A2), and (B1), the Heisenberg equation for σ is obtained as

$$\frac{d}{dt} \sigma = -\frac{\Gamma'}{2} \sigma - (2\sigma^\dagger \sigma - 1) \times [\sqrt{\Gamma_a} \tilde{a}_{-t}(0) + \sqrt{\Gamma_b} \tilde{b}_{-t}(0) + \sqrt{\Gamma_c} \tilde{c}_{-t}(0)], \quad (\text{B2})$$

where $\Gamma' = \Gamma + \gamma (= \Gamma_a + \Gamma_b + \Gamma_c)$. By taking the same procedures as in Appendix A, the m -point function for the output state $C_m(\mathbf{r}_m; t)$ is given in Eq. (A7) by replacing Γ with Γ' . Thus, the upper limit of the input pulse length for generating a single-photon state d_m is modified as $d_m = \sqrt{8/5\pi}/\Gamma'$. For example, a recent cavity-QED experiment attained $\Gamma/\gamma \sim 6$, where Γ and γ are the decay rates to the optical paths and the environment, respectively [14]. In this case, d_m has 15% error compared to the complete lossless case and should multiply d_m by a factor $\Gamma/\Gamma_L \sim 0.857$.

-
- [1] M. A. Nielsen and I. L. Chuang, *Quantum Computation and Quantum Information* (Cambridge University Press, Cambridge, UK, 2000).
- [2] N. Gisin, G. Ribordy, W. Tittel, and H. Zbinden, *Rev. Mod. Phys.* **74**, 145 (2002).
- [3] N. Gisin and R. Thew, *Nat. Photonics* **1**, 165 (2007).
- [4] B. Lounis and M. Orrit, *Rep. Prog. Phys.* **68**, 1129 (2005).
- [5] J. L. O'Brien *et al.*, *Nature (London)* **426**, 264 (2003).
- [6] R. Okamoto, H. F. Hofmann, S. Takeuchi, and K. Sasaki, *Phys. Rev. Lett.* **95**, 210506 (2005).
- [7] J. L. O'Brien, A. Furusawa, and J. Vučković, *Nat. Photonics* **3**, 687 (2009).
- [8] B. Darquié *et al.*, *Science* **309**, 454 (2005).
- [9] A. A. Houck *et al.*, *Nature (London)* **449**, 328 (2007).
- [10] M. Hofheinz *et al.*, *Nature (London)* **454**, 310 (2008).
- [11] C. Brunel, B. Lounis, P. Tamarat, and M. Orrit, *Phys. Rev. Lett.* **83**, 2722 (1999).
- [12] Y. He and E. Barkai, *Phys. Rev. A* **74**, 011803 (2006).
- [13] K. Koshino, *Phys. Rev. Lett.* **98**, 223902 (2007).
- [14] T. Aoki, A. S. Parkins, D. J. Alton, C. A. Regal, B. Dayan, E. Ostby, K. J. Vahala, and H. J. Kimble, *Phys. Rev. Lett.* **102**, 083601 (2009).
- [15] O. Astafiev *et al.*, *Science* **327**, 840 (2010).